James L. Foster
Dorothy K. Hall
NASA/Goddard Space Flight Center
Greenbelt, MD 20771

Multisensor Analysis of Hydrologic Features with Emphasis on the Seasat SAR

Synthetic aperture radar imagery of the Wind River Range area in Wyoming is compared to visible and near-infrared imagery of the same area.

Abstract: *Synthetic aperture radar (SAR) imagery of the Wind River Range area in Wyoming is compared to visible and near-infrared imagery of the same area. Data from the Seasat L-Band SAR and an aircraft X-Band SAR are compared to Landsat Return Beam Vidicon (RBV) visible data and near-infrared aerial photography and topographic maps of the same area. Visible and near-infrared data provide more information than the SAR data when conditions are optimum. However, the SAR penetrates clouds and snow, and data can be acquired day or night. Drainage density detail is good on SAR imagery because individual streams show up well due to riparian vegetation causing higher radar reflections which result from the "rough" surface which vegetation creates. In the winter image, the X-Band radar data show high returns resulting from cracks on the lake ice surfaces. High returns are also evident in the L-Band SAR imagery of the lakes due to ripples on the lake surfaces induced by wind. It is concluded that utilization of multispectral data (visible, near-infrared, and microwave (radar)) would optimize analysis of hydrologic features.*

Introduction

The intent of this study was to assess the information content of the Seasat synthetic aperture radar (SAR) by comparing the L-Band (23.5-cm wavelength) Seasat SAR data with X-Band (3.1 cm) aircraft SAR data, Landsat-3 return beam vidicon (RBV) data, U-2 color-infrared photography, and topographic maps. In this paper, a multispectral approach was employed for analysis of some hydrologic features in the Wind River Range, Wyoming. Emphasis is placed on the Seasat SAR because it provides a new data source. The capabilities of the Seasat SAR for hydrologic studies in the Wind River Range area could truly be assessed because data from several different sensors were available for comparison. For this reason, the Wind River Range was chosen for study. Imagery was acquired on the following dates: Seasat SAR, 31 July 1978; aircraft SAR, 30 March 1979; Landsat-3 RBV, 11 August 1978; and U-2 photography, 21 March 1976 and 21 June 1976. No ground truth data were available for comparison with the remotely-sensed data.

Study Area

The Wind River Range is located in west-central Wyoming (Figures 1 and 2). Precambrian metamorphic and plutonic rocks and limestone, sandstone, and granitic lithologies comprise the geology of the area. The climate varies with altitude, being semi-arid at the base of the range at approximately 1830 m (6000 feet), and alpine at the summits at an elevation of nearly 4265 m (14,000 feet). Precipitation averages 300 mm (12 inches) a year at the base and over 1525 mm (60 inches) on the highest peaks. Approximately

Photogrammetric Engineering and Remote Sensing,
Vol. 47, No. 5, May 1981, pp. 655-664.

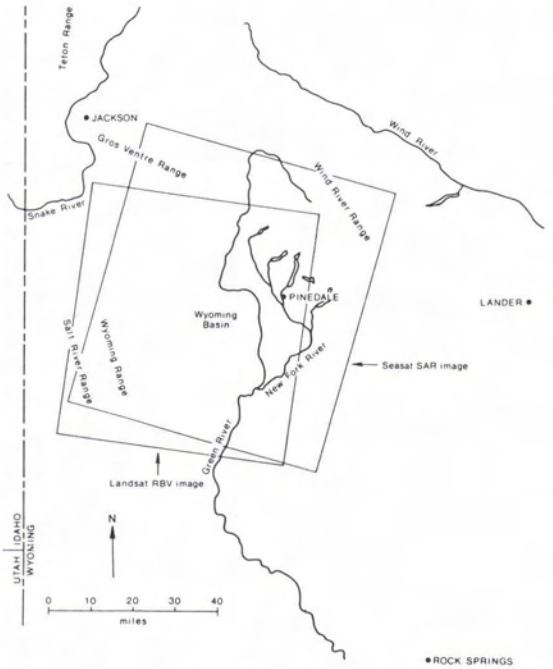

FIG. 1. Map of west-central Wyoming showing Seasat SAR and Landsat RBV image coverage.

two-thirds of this precipitation runs off as streamflow. As a result of the climate, latitude, and topography, there are 63 small valley glaciers in the Wind River Range, many of which are advancing.

The vegetation in the Wind River Range consists mainly of alpine meadows and herbaceous plants above 3050 m (10,000 feet). Below this elevation Douglas Fir are common near the base of the mountains, and Lodgepole Pine and Western Spruce-Fir forests dominate the higher slopes. Sagebrush, wheatgrass, and steppe vegetation can be found near the base of the mountains. In addition, cottonwood and willow trees are prevalent on the floodplains of many of the larger streams near the base of the mountain.

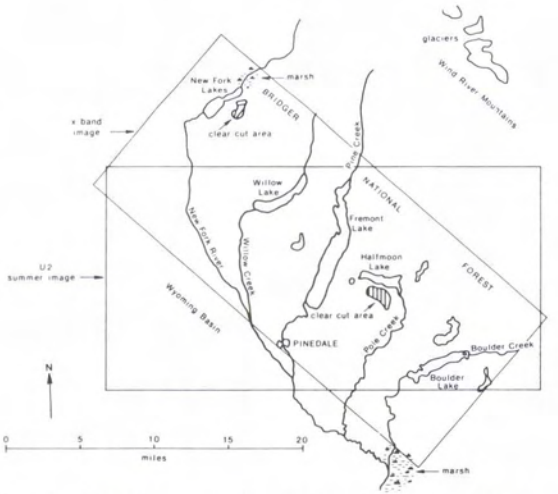

FIG. 2. Detailed map of a portion of Figure 1 showing X-band and U-2 image coverage.

SENSORS

L-BAND SAR (SEASAT)

The Seasat satellite was placed in a circular near-polar orbit in June of 1978. Seasat circled the Earth 14 times per day, completing 1503 revolutions prior to a power failure which terminated all remote-sensing capabilities in October of 1978. Synthetic aperture radar (SAR) imagery was acquired for brief periods when the satellite was in direct line-of-sight communication with one of the four receiving stations in North America or the receiving station in the United Kingdom. SAR imagery was acquired over most of the U.S., but total coverage of the continental land surfaces was not obtained.

A radar image is a record of the intensity of microwave energy reflected or scattered from each resolution cell. Like conventional radar, the SAR transmits electromagnetic pulses and records their return, or echo (Kovaly, 1978). The Seasat SAR antenna transmissions are spread over an angle of slightly less than 1.5°, which means that a given spot on the Earth's surface is within the beam for 2 seconds because the SAR is moving along its orbit at about 7.4 km/sec. Return echoes from each resolution element within this beam are integrated for a portion of that 2-second period so that each ground spot returns the radar beam from a range of angles. The synthetic aperture length which determines the azimuth resolution is the product of the orbital velocity of the satellite and the integration time. This results in an image having greater detail and better resolution than imagery from real aperture systems operating at the same altitude. In addition, the resolution of the imagery is independent of altitude. The Seasat SAR can be processed to yield an image which can resolve details as small as 25 m. The inherent azimuth resolution of a single fully focussed image is better than 7 m. However, to reduce scattering effects ("speckle") in the return signal, the signal is processed to a resolution approximately four times as great. Four such images are incoherently averaged to form the final product. The scale of the SAR imagery is approximately 1:450,000.

Radar has its own source of illumination and is therefore not restricted to daytime operation. Microwave signals at the Seasat SAR wavelengths are usually unaffected by clouds, fog, and atmospheric disturbances resulting in an all-weather measurement capability. Seasat SAR data result from horizontally like-polarized (HH) L-band (23.5 cm) radar

signals taken during ascending or descending orbital modes. The intensity or brightness of an individual resolution cell is related to backscattered energy from the source. More scattering will cause a brighter return. The surface parameters which have been found to affect the return signal are surface roughness, orientation, slope, and the complex dielectric constant (MacDonald and Waite, 1973). Incidence angle, polarization, and frequency are the instrument parameters which also affect the intensity or brightness of the return signal.

Relative surface roughness may be calculated by using the smooth and rough criteria of Peake and Oliver (1971). These criteria are,

for smooth surfaces: $h < \frac{\lambda}{8 \sin \gamma}$ for rough surfaces: $h > \frac{\lambda}{4.4 \sin \gamma}$

where h = the average height of surface irregularities (in cm),
λ = the radar wavelength (23.5 cm for Seasat SAR), and
γ = the depression angle between the horizontal plane and the radar wave incident upon the terrain (70° for Seasat SAR).

For the Seasat SAR the smooth criterion is calculated to be 3.1 cm, which means that surfaces with a vertical brief of 3.1 cm or less within the SAR footprint (25 m) will appear smooth and have a dark signature. The rough criterion is 5.7 cm, which means that surfaces with a vertical relief of 5.7 cm or more will appear rough and have a bright signature. Surfaces with vertical relief between 3.1 and 5.7 cm will have intermediate signatures (Sabins *et al.*, 1979).

The length of the electromagnetic wave with respect to the size of the terrain features determines whether a surface appears rough or smooth at that wavelength. A surface that is rough in the visible wavelengths may be quite smooth in the microwave wavelengths. A rough surface scatters the incident energy in all directions, returning some of it to the antenna. But a smooth surface reflects the incident energy in one direction, acting like a mirror. If the smooth surface happens to be perpendicular to the incident radar beam, then the energy returned to the antenna is intense. However, if the surface is at any other angle to the radar beam, none of the energy is returned (Moore, 1975).

Smooth surfaces of water are excellent specular reflectors. Because they are not viewed at right angles to the Seasat SAR, they specularly reflect all the microwave energy into space. Thus, on SAR imagery rivers and lakes having smooth surfaces usually appear black. Conversely, related horizontal and vertical surfaces, a building next to a road for example, may work together to form a corner reflector, returning a large part of the energy directly back to the antenna (Moore, 1975). Such surfaces on SAR imagery appear many times brighter than rough surfaces.

The dynamic range of the Seasat SAR system is low, corresponding to a maximum of six gray levels or spectral intervals. For this reason the more subtle variations in surface conditions are sometimes not seen. The Seasat SAR has a look angle of about 20° (the depression angle is about 70°) and incidence angles that commonly range between 0° and 30°. Surfaces normal to the radar look direction and having a slope angle larger than 20° may yield incidence angles of 0° and will be geometrically distorted due to the layover effect whereby foreslopes (closer to the antenna) appear foreshortened because the radar echo is returned sooner than echoes from the surrounding lower terrain (Matthews, 1975). Because of the scale of the Seasat imagery and the narrow radar beam width (6°), image distortion is not a serious problem. The corollary to layover of foreslopes is shadowing of backslopes, which occurs where the slopes are steeper than the depression angle (70°). In this study area most slopes do not approach 70°; consequently, most backslopes are not in radar shadow (Ford, 1979).

X-BAND SAR (AIRCRAFT)

The X-Band system used in this study is a synthetic aperture radar and is flown on-board the National Aeronautics and Space Administration RB-57 aircraft, typically at an altitude of 18,300 m (60,000 feet). This SAR images a swath of ~16.1 km (10 miles) on the ground. The instrument operates at a wavelength of ~3.1 cm (9600 ± 5 MHz) with a range and azimuth resolution of ~15.2 m (50 feet). Like (HH and VV) and cross-polarized (HV and VH) data are taken simultaneously. Data can be obtained in two modes. In mode I, the viewing angle (off-nadir) can be set between 14° and 51°. In mode II, the viewing angle can be set for any angle between 45° and 63° off-nadir. Viewing angles can be selected in the cockpit.

Comparison of the HH and VV with the HV and VH images of the same area show that the radar return signals are generally higher in the like-polarized imagery as seen in Figure 3. Mode I imagery gave higher returns than Mode II data, so only Mode I imagery is included in this analysis. Some banding is present in the imagery and hinders interpretation where it occurs.

The rough criterion for the X-Band SAR is calculated to be 1.1 cm, and the smooth criterion is 0.6 cm using the depression angle of 38.7°. The X-Band SAR depression angle is considerably less than that of the Seasat SAR (70°), and thus radar shadowing of backslopes is created in the resulting X-Band imagery.

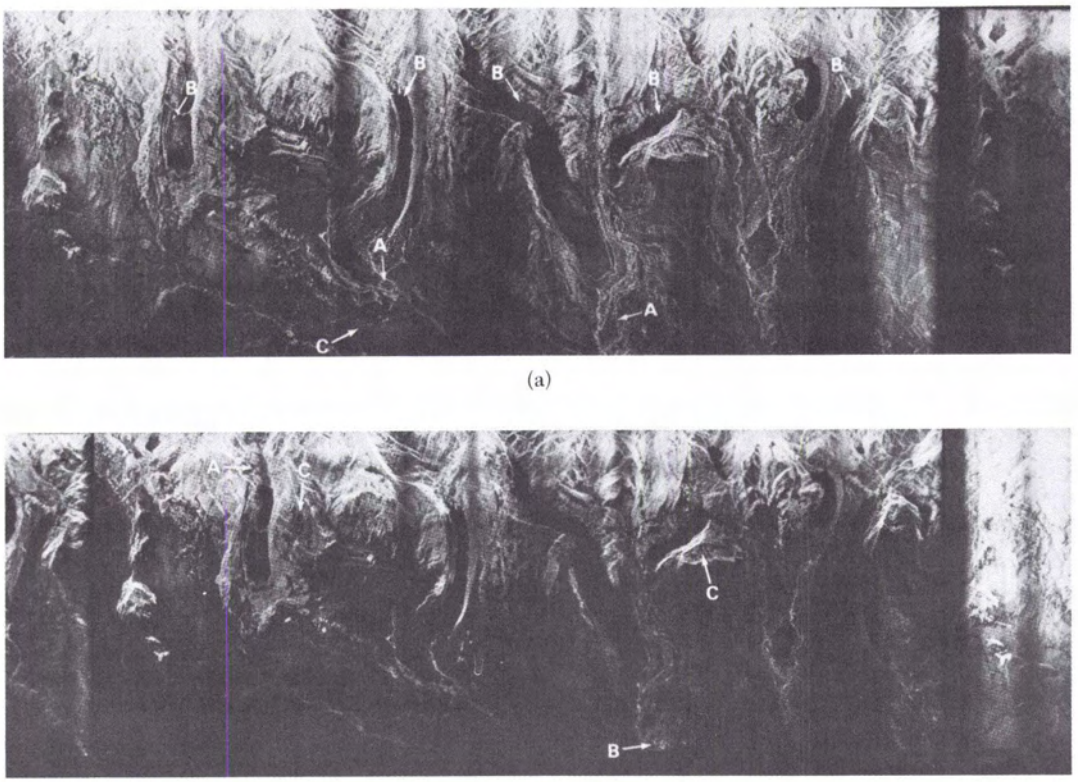

FIG. 3. (a) X-band SAR (VV) image taken 30 March 1978. (b) X-band SAR (VH) image taken 30 March 1978.

U-2 CAMERA

Aerial photography was taken over the Wind River Range as part of the NASA Earth Resources Aircraft Program (ERAP) from 1974 through 1976. Using an RC-8 camera on-board a U-2 aircraft, approximately 10-meter resolution imagery was obtained in the 0.5 μm to 1.1 μm spectral range. The U-2 aircraft photographs the Earth from an altitude of about 18,300 m (60,000 feet) with a focal length of 15 cm (6 inches). The scale of this high altitude photography is approximately 1:120,000.

LANDSAT RBV

Landsat imagery has been acquired over the Wind River Range since July of 1972 when Landsat-1 was first launched. Landsat-2 was launched in January of 1975 and Landsat-3 in March of 1978. The Landsat satellites have high resolution multispectral sensors, repetitive coverage capability, and cartographic fidelity. In addition to the multispectral scanner subsystem (MSS) on-board all three Landsat satellites, Landsat-3 also has a Return Beam Vidicon (RBV) system which employs two panchromatic vidicon cameras that operate in the 0.51 to 0.75 μm band. The RBV imagery has a nominal resolution of ~30 m and a scale of 1:500,000. Four overlapping Landsat-3 RBV subscenes comprise one MSS scene.

ANALYSIS AND RESULTS

The Seasat SAR image (Figure 4) was taken on 31 July 1978 in a descending orbital model (NE to SW). For this orbit the look direction is towards the NW. This scene shows the Wind River, Gros Ventre, and Wyoming Ranges of Wyoming and the Wyoming Basin. The bright or high return areas represent a high surface roughness within the SAR resolution element (25 m). Dark or low return areas represent smooth surfaces. The bright returns in the mountains are largely a result of the forest canopy covering the mountain slopes (for example, see area "A" on Figure 4). Forested areas have a high surface roughness; the forest canopy conceals the underlying surface by diffuse scattering of most of the radar energy.

Faults and lineaments within the mountainous areas can be easily detected on the SAR image as abrupt gray level changes as seen at "B" on Figure 4. Mountain slopes which face the look direction of the SAR reflect radar energy back to the antenna and produce brighter signatures than slopes facing away, which appear darker.

The Wyoming Basin appears dark in the center of the image as seen in Figure 4 marked "C". The relatively smooth terrain gives a low radar return and, as a result, rivers and streams within this low return region show up as high return or bright

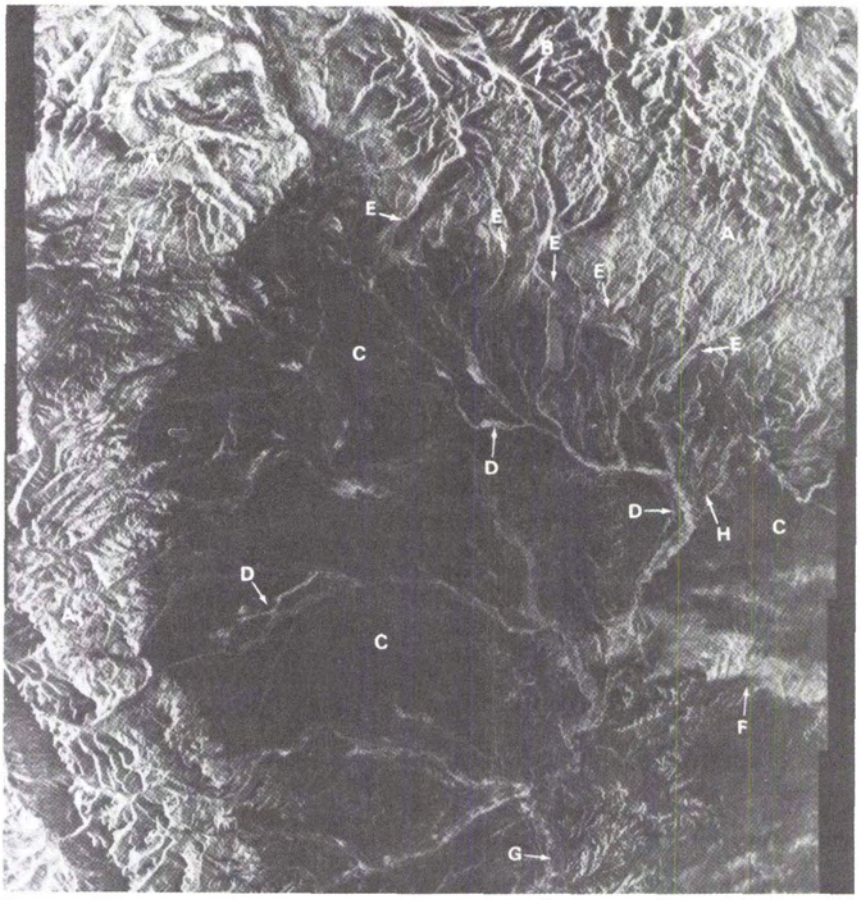

FIG. 4. Seasat SAR scene of west-central Wyoming taken on 31 July 1978. The look direction is towards the northwest.

features because of the vegetation confined to stream banks and floodplains having a high surface roughness relative to the non-vegetated surrounding plains (Sabins *et al.*, 1979). This can be seen in area "D" on Figure 4.

At the base of the Wind River Mountains, north of the New Fork River, several glacial lakes are visible on the Seasat image. The lakes vary in brightness from black to gray. Ripples and waves on the lake surfaces most likely produce higher returns and smooth, calm water produces lower returns (Sabins *et al.*, 1979). The lakes (areas marked "E" on Figure 4) will be discussed in more detail later.

The bright streaks in the lower right corner of the image (area F) are perhaps associated with precipitating clouds. Precipitation was recorded at several locations in west-central Wyoming on the day of the Seasat overpass, and the Geostationary Operational Environment Satellite (GOES) confirmed the presence of cumulonimbus cloud cells south of the Wind River Range at the same hour that the Seasat image was taken (9:00 P.M. local time). Landsat imagery, U-2 photography, and topographic and geologic maps of the same area do not indicate the presence of any surface features which could otherwise explain these returns. It is possible that these returns may be caused by differences in soil moisture resulting from precipitation which occurred earlier in the day.

The area of bright returns in the lower right hand center of the image (area "G") is non-vegetated but the rough (highly dissected) surface results in a high return of the scattered radar energy. A marsh area transitional in brightness between the vegetated stream channels and the dark basin areas can be seen at area "H" on Figure 4.

Dendritic drainage characterizes this part of Wyoming. The combination of high surface runoff and non-resistant and impermeable bedrock results in a highly dissected surface. The associated drainage features give high returns and thus appear bright on the radar imagery. The effect of radar layover, discussed earlier, tends to enhance small valleys which dissect ridges and slopes.

In the semi-arid climate which characterizes the basin area, vegetation is usually confined to stream banks and flood plains. This riparian veg-

etation provides a marked contrast to the non-vegetated interfluvial zones, thus making stream identification easier than in a more uniformly vegetated region. Though many of the rivers, streams, and tributaries occur on relatively flat plains, they show up on SAR imagery because of multiple radar reflections from the stream beds and associated vegetation having the effect of accentuating surface roughness (McCoy, 1967; Hall and Bryan, 1977). This is the case even though water in the channels gives no return.

Four orders of streams can be identified on the basin floor and on mountain slopes from the 1:450,000 scale Seasat image (Figure 4). More drainage information is discernable on mountain slopes which are in the look direction of the Seasat and X-Band radars because more energy is directly reflected back to the sensor. Typically, four orders of streams can be identified on the X-Band imagery (Figures 3a and b), although greater detail can be discerned in some well-dissected regions within the VV polarized data. For comparison, it should be pointed out that four stream orders can also be mapped using Landsat RBV imagery and USGS 1:250,000 scale topographic maps of the same area. On the 10-m resolution U2 imagery as many as six stream orders can be identified in some areas, and gullies and ditches can be easily located. A direct comparison between the X-Band SAR and the Seasat SAR at the same scale was not accomplished in the study because, when the Seasat image was photographically enlarged to the same scale as the X-Band image, a loss of image quality and detail resulted.

Due to the high spatial resolution of the X-Band radar (15 m) and the roughness criterion of 1.1 cm, canals and drainage diversions in the area to the south of Willow Lake and Fremont Lake can be discerned (Figure 3a, area "A"). Even though some of these canals and diversions are narrower than 15 m, the linearity of these features provides sufficient definition or contrast to allow their detection. Several lakes are present in the X- and L-Band radar scenes (Figure 3, area "B", and Figure 4, area "E"). Localized high returns in portions of the lakes can be seen on both of the images. The bright returns are caused by different factors in each case because the images were acquired during different seasons. On the Seasat SAR image, which was acquired during the summer, much of New Fork Lakes acts as a specular reflector and appears dark on the Seasat image. Other portions of New Fork Lakes give high returns due to ripples produced by wind action. This was inferred after analyzing meterological data from surface weather maps at the time of the Seasat overpass, which indicated wind speeds of about 5 m/s. Other lakes also give localized high returns, as seen in Figure 4 (Fremont and Willow Lakes). Ripples on the lake surfaces are rough at the Seasat SAR wavelength and cause high reflections. The bright returns may be partially attributed to the steep (~70°) depression angle of the Seasat SAR. The darker, low return edges of New Fork Lakes may have been protected from the wind during the satellite overpass and thus are not rough at the Seasat SAR wavelength.

A portion of the Seasat SAR scene was enlarged using the digital data on the Atmospheric and Oceanographic Interactive Processing System (AOIPS) at Goddard Space Flight Center. This was done in order to determine how much additional detail could be obtained by doing a 1:1 sampling of the lines comprising the SAR data. The resulting subscene was enhanced by contrast stretching the spectral limits of the data in the subscene, and assigning new spectral limits. The image product, shown in Figure 5, does not show any additional detail, but allows one to enhance features of interest for better comparison with other imagery and topographic maps.

At the time in which the X-Band image was acquired (30 March 1978) the lakes were completely ice-covered as determined through analysis of Landsat imagery. Localized bright returns within the lakes are particularly evident in the like polarized, VV, image as seen in Figure 3a, while the VH cross polarized imagery (Figure 3b) renders dark returns within the lakes. The localized bright returns are due to reflections from a rough ice surface, the snow/ice and ice/water interfaces, and possibly air bubbles and cracks in the near surface ice as discussed by Page *et al.* (1975).

Snow was on the ground when the X-Band image was acquired in March. In the mountain area, above the lakes, the snow depth varied from 1.0 to 3.0 metres. In the basin, below the lakes, the snow was 0.5 to 1.0 metres thick (USDA, 1979). Radar penetrates the snow and detects the ground surface beneath the snowcover at the X- and L-Band wavelengths (Waite and MacDonald, 1970). In the forested mountains, the tree canopy effectively camouflages the ground below because it reflects the microwaves before they can reach the snowcovered ground.

Glaciers and permanent snow fields are present in the highest elevations of the Wind River Range (Figure 2b). However, these features cannot be discerned on the Seasat SAR image even though mountain or valley type glaciers have been seen on other L-Band SAR imagery largely as a result of their morainal patterns. Also, valley glaciers are often heavily crevassed and represent a rough surface to the radar wavelength. In the Seasat SAR scene, Figure 4, the glaciers cannot be discerned from the surrounding terrain possibly because of their similarity in roughness to the terrain and the fact that they are alligned in a NW-SE direction

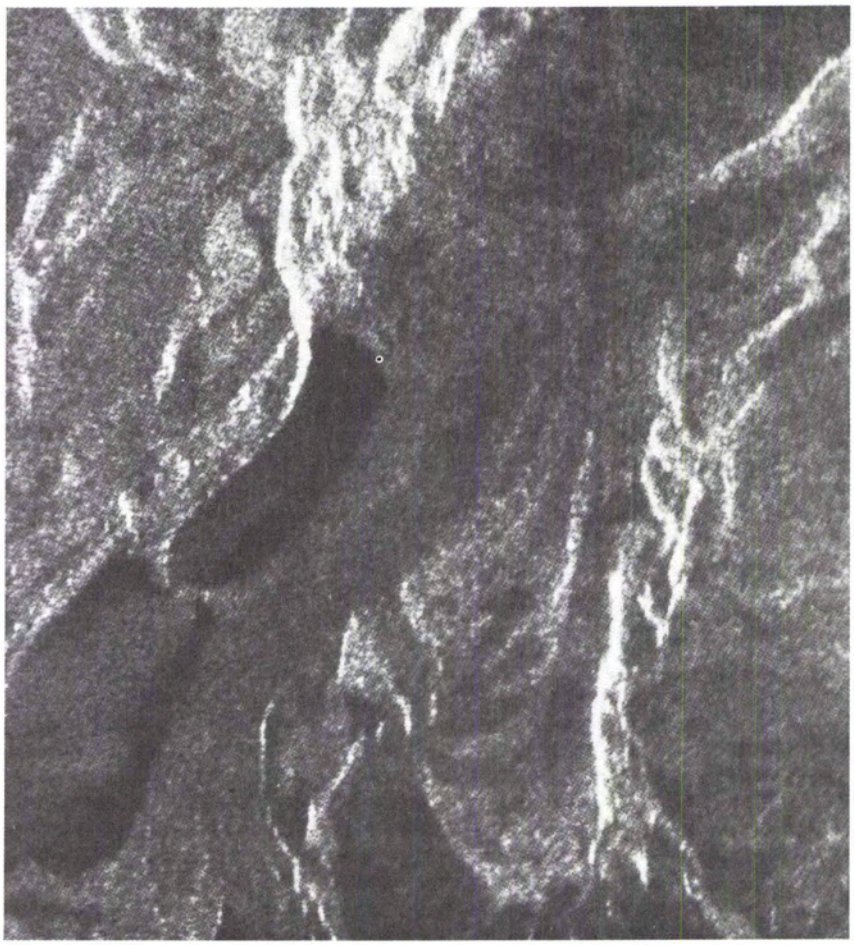

FIG. 5. Seasat SAR enlargement of New Fork Lakes subscene.

and are thus not in the optimal look direction to provide a signature response significantly different from that of the surrounding terrain.

On the Landsat RBV and U-2 images, contrary to radar images, snow and ice are often the most easily observable features. However, even with the Landsat and U-2 sensors, glaciers cannot be readily distinguished except in the late summer when the seasonal snowpack has melted. Figure 6a is a snowcovered U-2 scene taken in March of 1976. Compare this figure with Figure 3, which was taken in March of 1979 at which time the ground was also snowcovered. In the snowcovered U-2 scene there is a lack of detail of surface features compared to the detail in the radar image. The snow effectively conceals the underlying surface on the U-2 scene, but is penetrated by the radar. The utility of synthetic aperture radar in mapping many surface features does not appear to be seasonally dependent as are sensors which operate in the visible and near-infrared portions of the electromagnetic spectrum.

Because of differences in scale, resolution, and possibly spectral differences between the X-Band and Seasat SAR's, several features that were difficult to distinguish on Seasat were readily observable on the X-Band radar. For example, a marsh area is present in the north of New Fork Lakes where the New Fork River enters the upper lake (Figure 3a, area "A"). This marsh is characterized by relatively low vegetation such as rushes and willow shrubs. The resulting radar returns are transitional in roughness between a rough and a smooth surface. In the X-Band imagery, the marsh area is more easily seen in the cross polarized (Figure 3b) than in the like polarized imagery (Figure 3a) because the whole near nadir region is saturated in the like polarized imagery. The marsh area is not shown on the U-2 image. The town of Pinedale (Figure 3b, area "B") can be identified

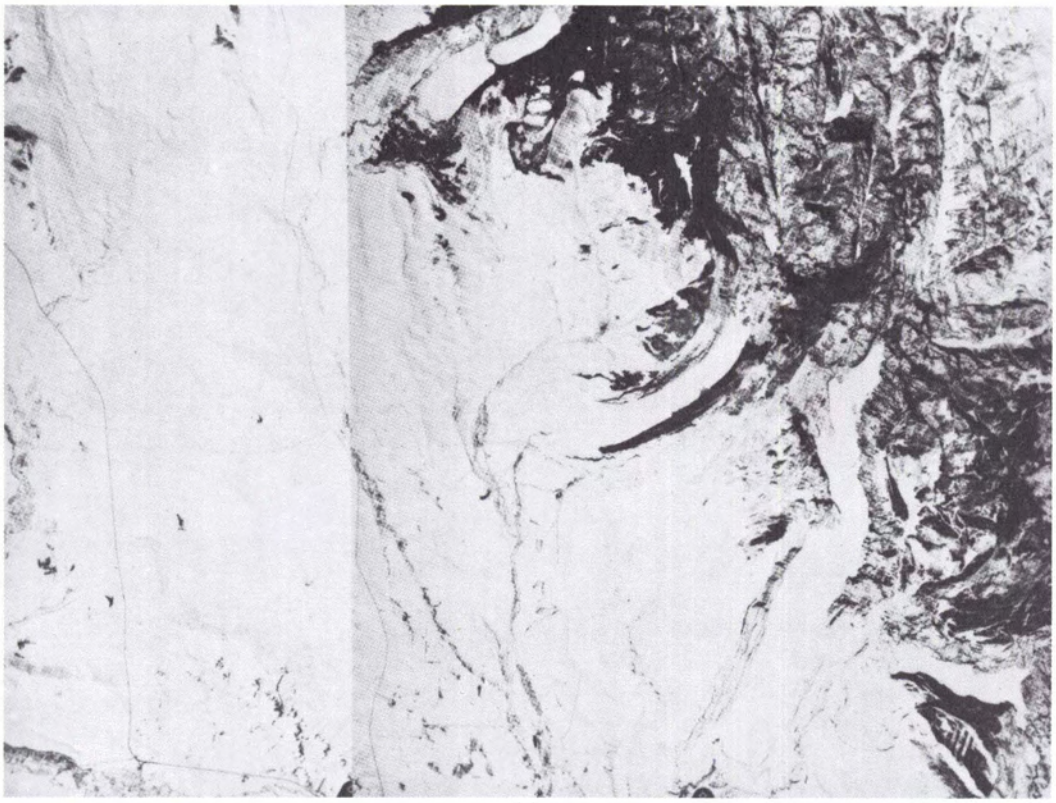

(a)

(b)

FIG. 6. (a) U-2 winter scene taken March 1976. (b) U-2 summer scene taken June 1976.

just to the south of Fremont Lake on the X-Band imagery. The bright returns are caused by differences in length and shape of the linear arrays of buildings that produce numerous corner reflectors (Ford, 1979). The striations and streams in the area below Willow Lake (Figure 3a, area "C") are thought to be cattle paths and jeep trails which result from the ranching activity in the area. In

addition, at area "C" on Figure 3b, a clear-cut area of conifers can be recognized. The bright stripes are trees that have not yet been harvested and the dark stripes are areas where almost all of the trees have been removed. These areas are relatively smooth and thus appear dark since they have no forest canopy. Another clear-cut area which is less distinguishable can be found just to the east of New Fork Lakes. On the Landsat RBV image (Figure 7), which is about the same scale as the Seasat SAR, the town of Pinedale is difficult to differentiate from the surrounding terrain; however, the clear-cut areas can be identified. On the U-2 image (Figure 6b) both the town of Pinedale and the clear-cut area are easily observable.

Conclusions

Based on the analysis of the Seasat image acquired over west-central Wyoming on 31 July 1978, it appears that the Seasat SAR does have a capability for hydrologic mapping, even though it was primarily designed for oceanographic applications. Both the L-Band (Seasat) and the X-Band (aircraft) SAR imagery were found to be useful for observing drainage detail. Streams have bright signatures on the SAR imagery because the riparian vegetation produces a rough surface and, thus, high radar returns. Lakes appear relatively bright on the Seasat image, presumably in response to surface ripples and waves induced by wind action. When the wind is calm the lakes act as specular reflectors and appear smooth or dark on the imagery. On the X-Band image, which was taken when the lakes were completely frozen, the lakes also have a bright signature because the ice surface is rough, probably as a result of fractures, rafting, and wind action during ice formation. SAR imagery did not reveal snow at either the 23.5-cm (L-Band) or 2.8-cm (X-Band) wavelengths. The radar penetrates through the dry snow to the underlying surface, and thus may be useful for analyzing the topography beneath the snowcover. In forested areas the tree canopy intercepts the radar signal and prevents it from reaching the snow surface.

Comparing Seasat and X-Band aircraft SAR imagery to Landsat RBV imagery, U-2 photography, and topographic maps of the Wind River Range area, it appears that the SAR data do not provide as wide a

Fig. 7. Landsat RBV image taken 11 August 1978.

range of hydrologic information as do the other sensors operating in the visible and near-infrared portions of the spectrum. Although the drainage detail extracted from the radar imagery is similar to that which can be extracted with the visible wavelengths, much more information regarding presence of snow can currently be acquired from the visible wavelengths than from L-Band and X-Band SAR. However, radar data, at longer wavelengths, are useful for analyzing hydrologic features beneath the snowcover, and at shorter wavelengths radar data may provide information concerning internal snowpack properties.

An important advantage of radar is its all-weather day/night remote sensing capability. The utility of radar for hydrologic studies is optimized during inclement weather, e.g., during a flood when conventional data cannot be acquired due to cloudcover or darkness. For future satellite missions designed for hydrologic studies, the multispectral approach using visible, near-infrared, infrared, and passive and active microwave (radar) wavelengths is obviously the optimum approach as opposed to using a single wavelength or sensor. It remains to be seen, however, if there is a synergistic effect on the overall results that would fully support the additional cost and complexity in the technology and data processing.

Acknowledgments

Dick Fenner and Doug LaPoint of NASA/Johnson Space Flight Center, Houston, Texas provided the C-130 aircraft radar data, and Frank Barath of the Jet Propulsion Laboratory, Pasadena, California provided the Seasat SAR data.

References

Ford, J. P., 1979. Analysis of Seasat Orbital Radar Imagery for Geologic Mapping in the Appalachian Valley and Ridge Province, Tennessee—Kentucky—Virginia. *Proc. of the Radar Geol. Workshop*, Snowmass, CO.

Hall, D. K., and M. L. Bryan, 1977. Multispectral Remote Observations of Hydrologic Features on the North Slope of Alaska. *Proc. of the Amer. Soc. of Photogrammetry Fall Tech-Mtg.*, 18-21 October, Little Rock, AR, pp. 393-424.

Kovaly, J. J., 1978. *Synthetic Aperture Radar.* Artech House, Inc. Dedham, MA, pp. 21-31.

MacDonald, H. C., and W. P. Waite, 1973. Imaging Radars Provide Terrain Texture and Roughness Parameters in Semi-arid Environments. *Modern Geol.* Vol. 4, No. 2, pp. 145-158.

Matthews, R. E. (ed.), 1975. *Active Microwave Workshop Report*, NASA SP-376, Washington, D.C., pp. 60-67.

McCoy, R. M. 1967. *An Evaluation of Radar Imagery as a Tool for Drainage Basin Analysis*, CRES. TR-61-31. Center for Research in Engin. Science, Univ. of Kansas.

Moore, R. K., 1975. Microwave Remote Sensors. In *Manual of Remote Sensing* (ed. R. G. Reeves), Vol. 1, pp. 399-537.

Page, D. F., and R. O. Ramsier, 1975. Application of Radar Techniques to Ice and Snow Studies. *Jour. Glac.*, Vol. 15, pp. 171-191.

Peake, W. H., and T. L. Oliver, 1971: *The Response of Terrestrial Surfaces at Microwave Frequencies.* Ohio State Univ. Electroscience Lab, Tech. Rep. AFAL-TR-70-301.

Sabins, F. F., R. Blom, and C. Elachi, 1979. Expression of San Andreas Fault on Seasat Radar Image. *Proc. of the Radar Geol. Workshop*, Snowmass, CO.

Simonett, D. S., 1978. *Active Microwave Applications Research and Development Plan.* Santa Barbara Remote Sensing Unit Technical Report 2.

U.S. Dept. of Agriculture, 1979. *Water Supply Outlook for Wyoming as of April 1, 1979*, Soil Conservation Service.

Waite, W. P., and H. C. MacDonald, 1970. Snowfield Mapping with K-Band Radar. *Remote Sensing of the Environment*, Vol. 1, No. 2, pp. 143-150.

(Received 14 February 1980; revised and accepted 28 October 1980)

Perspectives on Natural Resources Series—Symposium IV
The Arctic—Resource Development

Sir Sandford Fleming College
4-5 November 1981

For further information on this symposium on Arctic resource development and environmental concerns, please contact

Dr. Stephen H. Watts
Sir Sandford Fleming College, Frost Campus
P.O. Box 8000
Lindsay, Ontario K9V 5E6, Canada
Tele. (705) 324-9144